Magnetic field tunability of spin-polarized excitations in a high-temperature magnet

B. S. Holinsworth, H. Sims, J. G. Cherian, D. Mazumdar, N. C. Harms, B. C. L. Chapman, A. Gupta, S. A. McGill, and J. L. Musfeldt

Magnetic field tunability of spin-polarized excitations in a high-temperature magnet

B. S. Holinsworth,[1] H. Sims,[2,3] J. G. Cherian,[1] D. Mazumdar,[1] N. C. Harms,[1]
B. C. L. Chapman,[1] A. Gupta,[4] S. A. McGill,[5] and J. L. Musfeldt[1,6]

[1]*Department of Chemistry, University of Tennessee, Knoxville, Tennessee 37996 USA*
[2]*Department of Physics and Astronomy, Vanderbilt University, Nashville, Tennessee 37235 USA*
[3]*Materials Science and Technology Division, Oak Ridge National Laboratory, Oak Ridge, Tennessee 37831 USA*
[4]*Center for Materials for Information Technology,*
University of Alabama, Tuscaloosa, Alabama 35487 USA
[5]*National High Magnetic Field Laboratory, Florida State University, Tallahassee, Florida 32310, USA*
[6]*Department of Physics, University of Tennessee, Knoxville, Tennessee 37996 USA.*

We bring together magnetic circular dichroism, photoconductivity, and complementary first prin-
ciples calculations in order to unravel spin-charge interactions in the high Curie temperature magnet
$NiFe_2O_4$. Analysis uncovers a massive set of well-isolated spin down states, a metamagnetic tran-
sition involving spin on the Ni center that switches the electronic structure of this system, and
photoconductivity that depends on magnetic field. These findings open the door for the creation
and control of spin-polarized excitations from minority channel charge transfer in spinel ferrites.

I. INTRODUCTION

Magnetic semiconductors are at the heart of modern device physics. They naturally provide a non-zero magnetic moment below the ordering temperature, a spin-dependent band gap, and spin polarization that originates from exchange-coupled magnetization or an applied field creating a spin-split band structure.[1–5] Strongly correlated spinel ferrites are amongst the most noteworthy contenders for semiconductor spintronics.[5,6] $NiFe_2O_4$, in particular, displays spin-filtering, linear magnetoresistance, and wide application in the microwave regime.[6,7] This system is thus a superb research platform for exploring the role of interpenetrating magnetic sublattices on the charge channel excitations.

$NiFe_2O_4$ crystallizes in an inverse spinel structure (space group $Fd\bar{3}m$), where the Ni^{2+} cations occupy interstitial octahedral sites and the Fe^{3+} cations are equally distributed between octahedral and tetrahedral locations.[5,6] Antiferromagnetic coupling of the sublattices cancels the Fe moments while the Ni^{2+} spins remain uncompensated [Fig. 1 (a)][8] resulting in a theoretical net moment of $2\mu_B$ and $T_C = 850$ K.[9] Magnetic field drives a reorientation of the Ni spins at a critical field $B_{c(Ni)}$ of 0.3 T [Fig. 1 (b)].[9] The Fe spins presumably saturate at much higher fields ($B_{c(Fe)}$). Figure 1(c) displays the calculated density of states with well-known spin-split valence and conduction bands. The latter arises naturally from coupling of the two independent sublattices and suggests that $NiFe_2O_4$ may be able to support spin-polarized optical excitations.[5,10,11] Recent electronic structure calculations combined with linear optical spectroscopy revealed $NiFe_2O_4$ as an indirect gap material.[12] In fact, the 1.6 eV indirect gap along with the 2.4 and 2.8 eV direct gaps overlap the solar spectrum.[12] That said, questions have arisen[13] about the indirect nature of the 1.6 eV gap that require deeper investigation. Additionally, experimental evidence verifying (or refuting) key aspects of the predicted electronic structure[5,12] and clarifying the op-portunities that it presents is highly desirable.
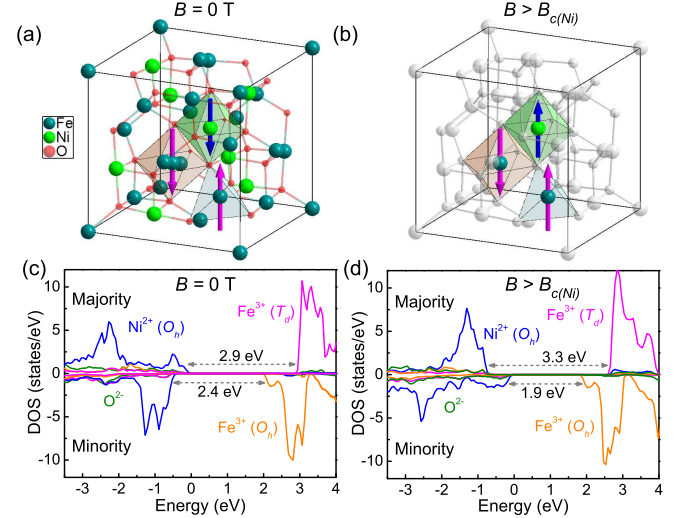

Figure 1. (Color online) (a, b) Crystal structure of $NiFe_2O_4$ showing the spin configuration at 0 T and above $B_{c(Ni)}$ where the Ni spin is flipped to align with the field. (c, d) Projected density of states (DOS) from hybrid functional calculations[12] depicting Ni $(O_h) \rightarrow$ Fe $(O_h$ and $T_d)$ charge transfer excitations in the minority and majority channels for the two spin configurations of interest.

In this work, we bring together magnetic circular dichroism (MCD), photoconductivity, and first-principles calculations with prior optical absorption spectroscopy[12] to unravel the electronic structure of $NiFe_2O_4$. Analysis reveals a large number of field-tunable states that can be attributed to minority channel excitations, significant spectral differences across the metamagnetic transition that are traced to coupling between the Ni spin orientation and the minority channel Ni $\rightarrow$ Fe charge transfer excitations, exchange splittings of 0.2 to 0.3 eV depending on the excitation, and enhanced photoconductivity between the two minority channel gaps under applied

field.Together these findings establish an energy window or "sweet spot" in the electronic structure that can be used for generating spin-polarized carriers with light and, at the same time, demonstrate how these excitations can be manipulated with magnetic field. These discoveries are important in the continuing race to generate, manipulate, and detect spin polarized currents and highlight new opportunities in the area of oxide electronics.[3,10,14,15]

II. METHODS

High-quality epitaxial $NiFe_2O_4$ films were grown on (001)-oriented $MgAl_2O_4$ substrates via pulsed laser deposition.[9] A 50 nm film was used for the MCD measurements, whereas a 200 nm film was employed for the photoconductivity work. MCD measurements were performed at the National High Magnetic Field Laboratory in transmission mode, using a 300 W Xe lamp, an 0.25 m monochromator, and a 10 T superconducting magnet. We carry out a "training run" over the full hysteresis loop before any data collection in order to "set the state", and the phase on the lock-in amplifiers is minimized at full field. That said, the sample has a hysteresis, so experimentally, the MCD response of the upsweep curve at 0 T minus that of the downsweep curve at 0 T is not zero. In other words, there is no such thing as a zero field state. To access the $\downarrow\downarrow\uparrow$ state, we apply $B > B_{c(Ni)}$. To access the $\downarrow\uparrow\uparrow$ state, we apply $B > B_{c(Ni)}$. Photoconductivity measurements were carried out using a setup equipped with a Xe lamp, a series of narrow bandpass filters, a high voltage source, tungsten probe tips, and a 1.5 T magnet. Sputtered platinum contacts were employed, and photoconductance was normalized with respect to the power density at each wavelength.

All calculations were performed using the Vienna *ab-initio* Simulation Package (VASP)[16] within the Perdew, Burke, and Ernzerhof (PBE)[17] generalized gradient approximation of density functional theory. We used the projector augmented-wave (PAW)[18] pseudopotential of Kresse and Joubert.[19] The Heyd, Scuseria, and Ernzerhof (HSE06)[20] method of hybrid-functional calculations were performed. We employed an $8 \times 8 \times 8$ Γ-centered **k**-mesh and a plane wave cutoff of 500 eV to ensure proper convergence of the wave functions. The exact-exchange portion of the hybrid calculations was performed on a coarser $4 \times 4 \times 4$ **k** grid to reduce the computational cost. Optical properties were determined by computing the imaginary part of the frequency-dependent dielectric function through summation over empty states, with the real part following from the Kramers-Kronig relation.

III. RESULTS AND DISCUSSION

A. Magneto-optical response of $NiFe_2O_4$

Figure 2(a) displays the MCD spectrum of $NiFe_2O_4$ in an applied field of ±10 T at 1.6 K. The linear absorption spectrum ($\alpha(E)$) is included for comparison, and the 1.6, 2.4, and 2.8 eV band gaps are indicated on the energy axis.[12] Examination of the spectra in Fig. 2(a) immediately reveals a large number of states below the majority channel gap. The local maxima in the dichroic response also coincide with inflection points in the absorption. This correspondence demonstrates an important derivative relationship that we discuss below.

MCD is a powerful tool for unveiling spin-dependent electronic structure because it probes the field-induced difference in the absorption between right and left circularly polarized light (RCP and LCP), often denoted as $+$ and $-$.[21–23] The magnitude of the dichroic response, I_{MCD}, can be expressed as:[22,23]
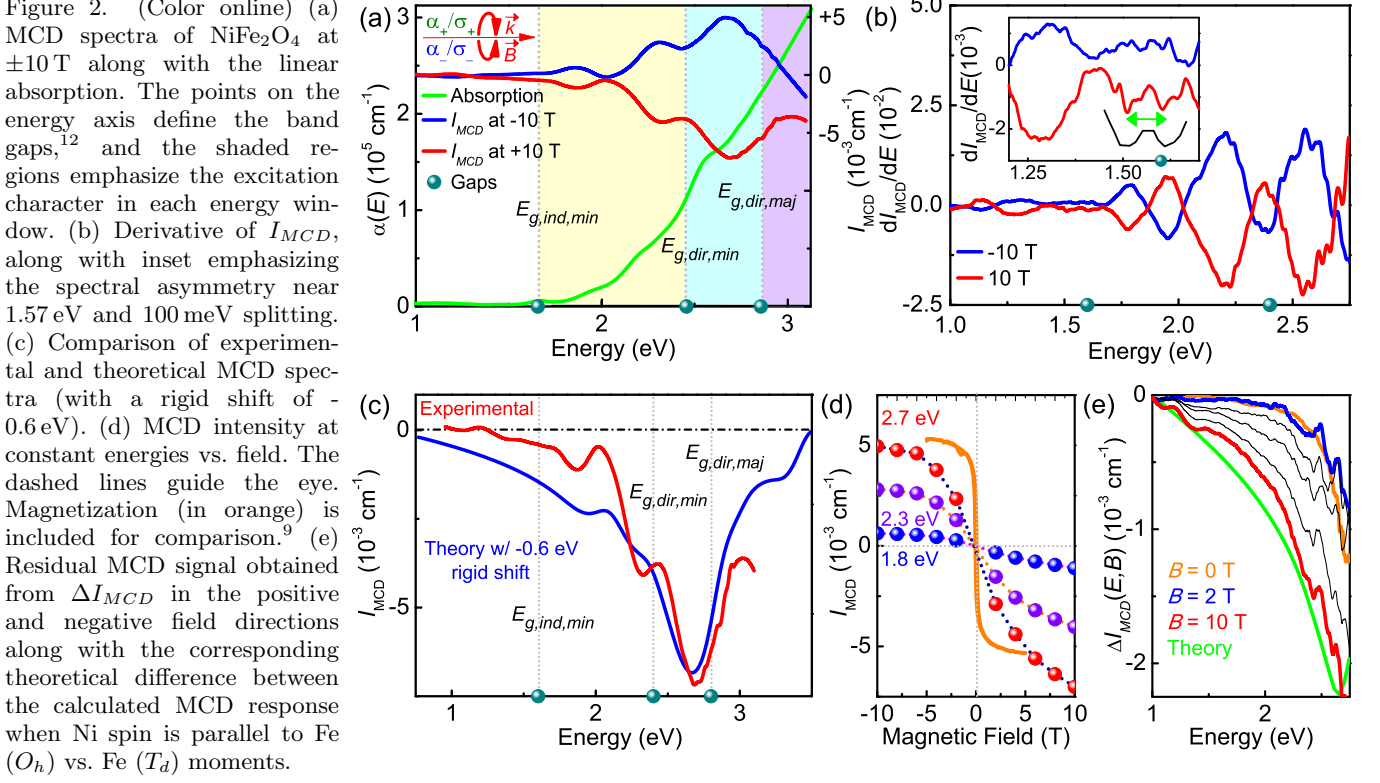
$$I_{MCD} \approx \frac{(\alpha_+(E) - \alpha_-(E))d}{2} \approx \frac{\Delta E}{2} \frac{1}{\alpha(E)} \frac{d\alpha(E)}{dE}. \quad (1)$$

Here, $\alpha(E)$ is the linear absorption, $d\alpha(E)/dE$ is the derivative of absorption with respect to energy, ΔE is the change in energy of the peak position, and d is the thickness of the film. Further, the resulting contrast in $\alpha_\pm(E)$ correlates with $\sigma_\pm$, the helicity.[22] This relationship shows a direct proportionality between I_{MCD} and $d\alpha(E)/dE$. Recalling that absorption is a joint density of states effect, the dichroic response will be related to critical points in the band structure, highlighting the link with the electronic structure. Complementary modeling of the dichroic response implemented the previously calculated matrix elements of the optical conductivity tensor[12] and the following expression for the MCD intensity:[24]

$$I_{MCD} \approx \frac{d\omega}{2c}\Im(n_+ - n_-) \approx \frac{2\pi h}{c}\Im[\frac{\sigma_{xy}}{(1 + i\frac{4\pi}{\omega}\sigma_{xx})^{1/2}}]. \quad (2)$$

Here, $n_\pm = (\epsilon_{xx} \pm \epsilon_{xy})^{1/2}$ is the refractive index of RCP (or LCP) light arising from the dielectric function ϵ, h is film thickness, and c is the speed of light. Different spin configurations were employed to simulate the effect of magnetic field.

Returning to the spectra in Fig. 2(a), we see that the derivative-like features in the dichroic response of $NiFe_2O_4$ can be assigned based upon an understanding of the band structure and projected density of states.[12] Importantly, there are a large number of features in the 1.5 to 2.8 eV energy window - where only minority channel charge transfer excitations are active. This is strong evidence for spin-polarized excitations. Spectral features emanating from on-site d-to-d excitations are also apparent.[25,26] In addition to being a sensitive technique for locating important features in the density of states, dispersions in the MCD spectra give reliable estimates of the spin splitting between majority and minority bands.

Figure 2. (Color online) (a) MCD spectra of NiFe$_2$O$_4$ at ±10 T along with the linear absorption. The points on the energy axis define the band gaps,[12] and the shaded regions emphasize the excitation character in each energy window. (b) Derivative of I_{MCD}, along with inset emphasizing the spectral asymmetry near 1.57 eV and 100 meV splitting. (c) Comparison of experimental and theoretical MCD spectra (with a rigid shift of -0.6 eV). (d) MCD intensity at constant energies vs. field. The dashed lines guide the eye. Magnetization (in orange) is included for comparison.[9] (e) Residual MCD signal obtained from ΔI_{MCD} in the positive and negative field directions along with the corresponding theoretical difference between the calculated MCD response when Ni spin is parallel to Fe (O_h) vs. Fe (T_d) moments.

We find exchange splittings in the range of 0.2 to 0.3 eV depending upon the excitation, in reasonable agreement with theoretical predictions.[5,6]

Figure 2(b) displays the derivative of the MCD spectrum as a function of energy. This rendering shows how gap energies correspond to local extrema in dI_{MCD}/dE at 1.6, 2.4, and 2.8 eV. Another important energy scale, missed previously, appears at ≈1.8 eV. dI_{MCD}/dE in the region near the indirect gap is especially interesting.[27] A doublet structure centered at 1.57 eV, emphasized by the black line, is clearly observed in the data taken at +10 T, whereas in the opposite (-10 T) field direction, the doublet is absent. The total splitting of this doublet in the spin down channel is 100 meV. Dividing by two yields the mediating phonon energy of 50 meV - matching nicely with the O-Fe-O bending mode.[12] Furthermore, this doublet does not have a node. Since a single angular momentum of light is being absorbed in the relevant energy window, we conclude that the fundamental gap excitation is spin polarized.[21] We attribute this finding to the spin-split band structure and the two distinct symmetry environments of the Fe centers.

Figure 2(c) compares the experimental MCD spectrum of NiFe$_2$O$_4$ with that calculated using Eqn. 2. Here, the theoretical curve has been rigidly shifted to account for over-estimation of the band gap within the hybrid functional method.[12] The excellent overall agreement between the measured and calculated spectra immediately verifies that the theoretical MCD response captures the essential aspects of the electronic structure. This is em-

phasized by critical points in the band structure.

Figure 2(d) displays constant energy cuts of the dichroic response vs. magnetic field. The resulting curves display a non-linear progression akin to magnetization,[9,28] although saturation occurs much more slowly due to the local nature of this probe[29] and with some asymmetry compared with $M(B)$ that is accounted for by the metamagnetic transition (discussed below). Optical tracking of $M(B)$ is extremely important for optical data storage and advanced sensing.[30] It is therefore striking that constant energy cuts of the dichroic response reveal such a correlation - even as new types of excitations are accessed under magnetic field. Figure 2(e) displays ΔI_{MCD} for the two different field directions (±B). The difference expressed by the $B = 0$ T curve is due to sample hysteresis. The contrast grows with increasing energy and applied field reaching values of -2.5×10^{-3} cm^{-1} at 2.75 eV and 10 T.

Detailed analysis of the electronic structure under different spin configurations provides a striking account of ΔI_{MCD}. Recall that the excitation spectrum in ordinary ferromagnets, e.g. iron, does not depend on field direction: all states "flip" their spin under applied field, giving equal access to transitions. Introducing a second magnetic sublattice does not in itself change this picture. However, in NiFe$_2$O$_4$, and indeed in other inverted spinels, two transition metal centers comprise one sublattice, and the spins associated with the Ni ions change polarization across $B_{c(Ni)}$. Comparison of the predicted partial densities of states [Fig. 1 (c,d)] reveals precisely

how the metamagnetic transition modifies the electronic structure. While the density of states associated with the Fe centers remains fairly rigid and relatively insensitive to changes in the microscopic spin arrangement, that associated with Ni^{2+} is modified significantly. In fact, these bands move from the majority (minority) to minority (majority) channel as the Ni spin flips, providing carriers in the Ni states access to a completely different set of spin-allowed charge transfer excitations.[3] As a result, the MCD spectrum of $NiFe_2O_4$ is altered dramatically across $B_{c(Ni)}$. This is the origin of ΔI_{MCD}.

Naturally, we sought to predict how the metamagnetic transition affects the electronic structure. MCD spectra computed for the field-induced state ($B > \pm B_{c(Ni)}$) show two primary differences when compared to the ground state ($B = 0$). First, all features shift to higher energies (e.g. 70 meV for the 2.7 eV excitation). Second, intensity is lost below ≈ 3.3 eV, at which point the spectra begin to develop qualitative differences. Close inspection of the spectra in Fig. 2(a) reveals peak position offsets of about 50 meV, in excellent agreement with these predictions. Moreover, a simple difference between the MCD spectra calculated in the two states is a very close and parameter-free match with the experimental value of ΔI_{MCD} in Fig. 2(e). We therefore conclude that this spectral asymmetry arises from electronic structure differences between the ground state and that of $B > B_{c(Ni)}$. Experimentally, this corresponds to -10 T and 10 T as shown in Fig. 1.

B. Photoconductivity of $NiFe_2O_4$

To provide additional information on the interplay between charge and spin, we measured the photoconductivity of $NiFe_2O_4$ [Fig. 3(a)]. This property derives from the creation of electron-hole pairs with light: $\sigma_{PC} \propto \eta\alpha(E)\tau$. Here, σ_{PC} represents the photoconductance, η is the carrier generation probability, $\alpha(E)$ is the absorption coefficient, and τ is the carrier lifetime. Comparing σ_{PC} and $\alpha(E)$ reveals that photoconductivity begins to develop near the fundamental gap at 1.6 eV - evidence that there are important electronic states in the energy window below the 2.8 eV direct gap. This window of electronic states arises from the two discrete symmetry environments of the Fe centers and is well modeled in our previous work.[31] Figure 3(b) displays typical current vs. voltage (I-V) curves with white light on and off. The data in panel (a) were obtained from similar I-V curves collected at specific illumination wavelenghts (and converted to energy for comparison with the absorption curve).

Application of a magnetic field provides an opportunity to further explore the photo-excited minority channel carriers. Figure 3(c) displays a typical set of I-V curves taken at 2.0 eV. As a reminder, light at this energy excites Ni $O_h \rightarrow$ Fe O_h charge transfer in the minority channel. The illumination and magnetic field conditions are indicated as ($h\nu$, B). Using I-V curves like those in Fig. 3(c), we determined field-induced changes

in photoconductivity. Figure 3(d) summarizes these findings by plotting them as magnetoresistances. It is immediately apparent that $NiFe_2O_4$ exhibits strong field effects (-6.5%) in the range where only minority carriers are active. Furthermore, this response is well above the standard magnetoresistance (on the order of -1%).[7,32] We conclude that light and field together are more effective than field alone - at least in the energy window between the minority channel indirect and direct gaps.
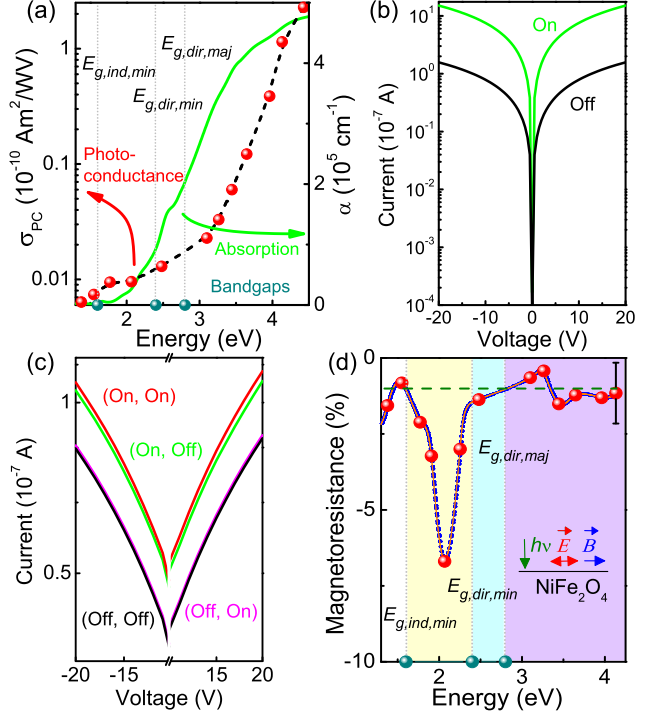

Figure 3. (Color online) (a) Photoconductance of $NiFe_2O_4$ measured at a series of illumination energies compared with the absorption spectrum. (b) Example I-V curves taken using a broadband xenon lamp. (c) Example I-V curves using a combination of light (2.0 eV) and magnetic field (≈ 1.5 T) as indicated. Magnetoresistance measurements for the light off state are included for completeness. (d) Field-induced changes in photoconductivity are displayed as magnetoresistance. The blue line guides the eye. The teal dots on the energy axis indicate band gap positions, the shaded regions emphasize the character of the excitations in each energy window, and the dashed horizontal dark green line denotes the intrinsic magnetoresistance.[7] The schematic shows the measurement geometry.

The effects discussed here differ significantly from those that arise in dilute magnetic semiconductors and many of the chalcogenides. The unusual electronic properties of the former are generally attributed to impurity band interactions,[22,28] whereas the latter emanate from strong spin-orbit coupling and include spin-split bands, Rashba splitting, and topologically-protected surface states.[33,34] The character of $NiFe_2O_4$'s spin-polarized excitations instead emerges from the two independent magnetic sublattices - an aspect of the crystal, chemical, and

electronic structure that will be replicated (in some form) in other spinel ferrites. These materials, already well known for their high Curie temperatures and robust moments, should be explored for enhanced electronic effects, with additional advantages if the active energy window has a healthy overlap with the solar spectrum.

IV. CONCLUSION

In summary, we combined magnetic circular dichroism, photoconductivity, and first principles calculations with prior optical absorption to unravel the character of the minority channel excitations in $NiFe_2O_4$ and to test whether spinel ferrites can generate spin-polarized carriers. Analysis uncovers well-isolated spin down states, a metamagnetic transition involving Ni center spins that switches the electronic structure of this system, and photoconductivity that depends upon magnetic field. These findings demonstrate that spin-polarized current can be created by light in the energy window defined by the minority channel charge transfer excitations. We also point out that $NiFe_2O_4$ is expected to display a magnetically-driven transition to the fully polarized state involving saturation of the Fe spins at even higher fields. According to our calculations, even greater magneto-optical con-

trast should be anticipated across this transition,[35] making it an interesting area for future investigation. These discoveries open the door for the creating and controlling spin-polarized excitonic components from minority channel charge transfer in spinel ferrites.

V. ACKNOWLEDGMENTS

[1] D. D. Awschalom and M. E. Flatté, Nat. Phys. **3**, 153 (2007).

[2] R. Jansen, Nat. Mater. **11**, 400 (2012).

[3] H. Y. Hwang, Y. Iwasa, M. Kawasaki, B. Keimer, N. Nagaosa, and Y. Tokura, Nat. Mater. **11**, 103 (2012).

[4] J. S. Moodera, G.-X. Miao, and T. S. Santos, Phys. Today **63**, 46 (2010).

[5] N. M. Caffrey, D. Fritsch, T. Archer, S. Sanvito, and C. Ederer, Phys. Rev. B **87**, 024419 (2013).

[6] U. Lüders, M. Bibes, K. Bouzehouane, E. Jacquet, J.-P. Contour, S. Fusil, J.-F. Bobo, J. Fontcuberta, A. Barthélémy, and A. Fert, Appl. Phys. Lett. **88**, 082505 (2006).

[7] C. Jin, Q. Zhang, W. B. Mi, E. Y. Jiang, and H. L. Bai, J. Phys. D: Appl. Phys. **43**, 385001 (2010).

[8] J. B. Goodenough, *Magnetism and chemical bond*, Vol. 1 (Interscience Publ., 1963).

[9] J. X. Ma, D. Mazumdar, G. Kim, H. Sato, N. Z. Bao, and A. Gupta, J. Appl. Phys. **108**, 063917 (2010).

[10] P. V. Lukashev, J. D. Burton, A. Smogunov, J. P. Velev, and E. Y. Tsymbal, Phys. Rev. B **88** (2013).

[11] D. Xiao, G.-B. Liu, W. Feng, X. Xu, and W. Yao, Phys. Rev. Lett. **108** (2012).

[12] Q. C. Sun, H. Sims, D. Mazumdar, J. X. Ma, B. S. Holinsworth, K. R. O'Neal, G. Kim, W. H. Butler, A. Gupta, and J. L. Musfeldt, Phys. Rev. B **86**, 205106 (2012).

[13] C. Klewe, M. Meinert, A. Boehnke, K. Kuepper, E. Arenholz, A. Gupta, J.-M. Schmalhorst, T. Kuschel, and G. Reiss, J. Appl. Phys. **115**, 123903 (2014).

[14] S. Bader and S. Parkin, Annu. Rev. Condens. Matter Phys. **1**, 71 (2010).

[15] A. P. Ramirez, Science **315**, 1377 (2007).

[16] G. Kresse and J. Furthmüller, Computational Materials Science **6**, 15 (1996).

[17] J. P. Perdew, K. Burke, and M. Ernzerhof, Phys. Rev. Lett. **77**, 3865 (1996).

[18] P. E. Blöchl, Phys. Rev. B **50**, 17953 (1994).

[19] G. Kresse and D. Joubert, Phys. Rev. B **59**, 1758 (1999).

[20] J. Heyd, G. E. Scuseria, and M. Ernzerhof, J. Chem. Phys. **118**, 8207 (2003).

[21] G. A. Gehring, M. S. Alshammari, D. S. Score, J. R. Neal, A. Mokhtari, and A. M. Fox, J. Magn. Magn. Mater. **324**, 3422 (2012).

[22] M. Dobrowolska, K. Tivakornsasithorn, X. Liu, J. K. Furdyna, M. Berciu, K. M. Yu, and W. Walukiewicz, Nat. Mater. **11**, 444 (2012).

[23] W. D. Rice, P. Ambwani, M. Bombeck, J. D. Thompson, G. Haugstad, C. Leighton, and S. A. Crooker, Nat. Mater. **13**, 481 (2014).

[24] M. Amft, T. Burkert, B. Sanyal, and P. Oppeneer, Physica B **404**, 3782 (2009).

[25] K. Ohgushi, Y. Okimoto, T. Ogasawara, S. Miyasaka, and Y. Tokura, J. Phys. Soc. Jpn. **77**, 034713 (2008).

[26] V. Kocsis, S. Bordács, J. Deisenhofer, K. Ohgushi, Y. Kaneko, Y. Tokura, and I. Kézsmárki, Submitted (2017).

[27] J. Donecker and J. Kluge, Phys. Status Solidi B **77**, 243 (1976).

[28] M. A. Meeker, B. A. Magill, G. A. Khodaparast, D. Saha, C. J. Stanton, S. McGill, and B. W. Wessels, Phys. Rev.

B **92**, 125203 (2015).

[29] S. Manz, M. Matsubara, T. Lottermoser, J. Büchi, A. Iyama, T. Kimura, D. Meier, and M. Fiebig, Nat. Photonics **10**, 653 (2016).

[30] I. Žutić, J. Fabian, and S. D. Sarma, Rev. Mod. Phys. **76**, 323 (2004).

[31] Q. C. Sun, C. S. Birkel, J. Cao, W. Tremel, and J. L. Musfeldt, ACS Nano **6**, 4876 (2012).

[32] Z. Quan, W. Liu, X. Li, X. Xu, K. Addison, D. Score, and G. Gehring, Mater. Lett. **65**, 2982 (2011).

[33] C. L. Kane and E. J. Mele, Phys. Rev. Lett. **95** (2005).

[34] G. Aivazian, Z. Gong, A. M. Jones, R.-L. Chu, J. Yan, D. G. Mandrus, C. Zhang, D. Cobden, W. Yao, and X. Xu, Nat. Phys. **11**, 148 (2015).

[35] See Supplemental Material at [URL will be inserted by publisher] for theoretical details.